

Article

Not peer-reviewed version

Assessment of Control Effectiveness for the Invasive Species *Spartina alterniflora* in the Yellow River Delta

[Huiying Li](#) , [Guoli Cui](#) , Haojie Liu , Qi Wang , Sheng Zhao , [Xiao Huang](#) , [Rong Zhang](#) * , [Mingming Jia](#) , [Dehua Mao](#) , [Hao Yv](#) , [Zongming Wang](#) , [Zhiyong Lv](#)

Posted Date: 2 December 2024

doi: 10.20944/preprints202412.0002.v1

Keywords: *Spartina Alterniflora*; Zhuhai-1 Hyperspectral Image; U-Net; Relief-F



Preprints.org is a free multidisciplinary platform providing preprint service that is dedicated to making early versions of research outputs permanently available and citable. Preprints posted at Preprints.org appear in Web of Science, Crossref, Google Scholar, Scilit, Europe PMC.

Copyright: This open access article is published under a Creative Commons CC BY 4.0 license, which permit the free download, distribution, and reuse, provided that the author and preprint are cited in any reuse.

Article

Assessment of Control Effectiveness for the Invasive Species *Spartina alterniflora* in the Yellow River Delta

Huiying Li ^{1,2}, Guoli Cui ^{1,2}, Haojie Liu ¹, Qi Wang ^{1,2}, Sheng Zhao ¹, Xiao Huang ³, Rong Zhang ^{2,*}, Mingming Jia ², Dehua Mao ², Hao Yu ⁴, Zongming Wang ² and Zhiyong Lv ⁵

¹ School of Environmental and Municipal Engineering, Qingdao University of Technology, Qingdao 266520, China;

² State Key Laboratory of Black Soils Conservation and Utilization, Northeast Institute of Geography and Agroecology, Chinese Academy of Sciences, Changchun 130102, China

³ Department of Environmental Sciences, Emory University, Atlanta, GA 30322, USA

⁴ Modern Industry College, Jilin Jianzhu University, Changchun 130118, China;

⁵ School of Computer Science and Engineering, Xi'an University of Technology, Xi'an 710054, China

* Correspondence: zhangrong@iga.ac.cn

Abstract: Coastal wetlands are critical for global biodiversity and ecological stability, yet the invasive *Spartina alterniflora* (*S. alterniflora*) poses severe threats to these ecosystems. This study evaluates the effectiveness of management efforts targeting *S. alterniflora* in the Yellow River Delta (YRD) using Zhuhai-1 hyperspectral imagery and the U-Net method. The U-Net model, coupled with the Relief-F algorithm, achieved superior extraction accuracy (Kappa > 0.9, overall accuracy 93%) compared to traditional machine learning methods. From 2019 to 2021, *S. alterniflora* expanded rapidly, increasing from 4,055.06 hm² to 6,105.50 hm², primarily in tidal flats and water bodies. A clearing project reduced its extent to 5,063.62 hm² by 2022, and by 2023, only 0.55 hm² remained. These results underscore the effectiveness of Shandong's management policies but highlight the risk of regrowth due to the species' resilience. Continuous monitoring and maintenance are essential to prevent resurgence and ensure wetland restoration. This study offers critical insights into dynamic vegetation monitoring and informs conservation strategies for wetland health.

Keywords: *S. alterniflora*; Zhuhai-1 hyperspectral imagery; U-Net; Relief-F

1. Introduction

Coastal wetlands are vital ecosystems that protect shorelines, support biodiversity, improve water quality, and store carbon, making them crucial for both environmental health and human well-being [1,2]. However, as ecologically sensitive areas, coastal wetlands are particularly susceptible to invasion by alien species—a susceptibility further exacerbated by increased human activity and global environmental changes [3]. *S. alterniflora*, commonly abundant in the coastal areas of the Atlantic, was introduced into China in the 1980s for coastal ecosystem restoration purposes [4,5]. The invasion of *S. alterniflora* harms coastal wetlands by outcompeting native species [3], altering hydrology, reducing biodiversity, and degrading critical habitats for wildlife [6]. Recognizing its threat, *S. alterniflora* was successively listed in the "First Batch of Invasive Alien Species in China" in 2003 and the "Catalogue of Key Managed Invasive Alien Species" in 2023 [7].

To address this issue, The National Forestry and Grassland Administration, along with four other ministries and relevant departments of the State Council, formulated the "Special Action Plan for the Control of *S. alterniflora* (2022-2025)" (referred to as the "Plan"). The Plan aims to achieve effective nationwide management of *S. alterniflora* by 2025, with each province attaining a removal rate of over 90%. Therefore, rapidly, accurately, and comprehensively understanding the dynamics of *S. alterniflora* removal and its management effectiveness is crucial. This knowledge provides essential baseline information for the controlling and managing of *S. alterniflora*, instrumental in

formulating scientific policies that protect ecological security and promote the sustainable development of coastal wetlands.

Monitoring *S. alterniflora* is challenging due to its rapid spread, dense growth, and the vast and often inaccessible coastal areas it occupies [8,9]. Remote sensing technology allows for efficient and accurate tracking of *S. alterniflora* over large areas, providing critical insights for effective management and control strategies [10,11]. Early remote sensing applications on *S. alterniflora* detection primarily relied on optical imagery with medium spatial resolution, such as Landsat MSS/TM/ETM+/OLI [12–14] and SPOT-1/2/3 [15–17]. While these methods offered valuable insights, they were sometimes limited due to constraints in spatial resolution and weather conditions. With the deployment of high-resolution satellite sensors, researchers have achieved more detailed monitoring of *S. alterniflora* in coastal areas of China, including the YRD [18,19], Pearl River Delta [20,21] and Zhangjiang Estuary [22]. This has resulted in more precise mapping and enhanced management of its invasion. However, high-resolution data in *S. alterniflora* mapping may face limitations including high cost, large data volumes, and challenges in differentiating between species in densely vegetated areas [23]. Recent innovations, including multispectral and hyperspectral imaging, have further enhanced the capacity to distinguish *S. alterniflora* from native vegetation and accurately monitor its distribution [24,25]. Advancements in satellite technology and miniaturization have made hyperspectral imaging more accessible, with compact sensors now being used on drones and small satellites [26]. The Zhuhai-1 hyperspectral satellite represents a significant milestone in this progression. By providing high-resolution, detailed spectral data, Zhuhai-1 enhances our ability to monitor and analyze the change characteristics of *S. alterniflora* with greater accuracy. Its data is crucial for applications such as coastal environment monitoring, offering valuable insights that support effective decision-making and resource management.

In addition to the resolution of sensor, the effectiveness of image processing techniques and algorithms, further impact the precision of the interpretation. Research on remote sensing methods for identifying *S. alterniflora* has progressed from traditional pixel-based approaches [14] to advanced techniques, including Object-Based Image Analysis [27], and machine learning algorithms like Support Vector Machines (SVM) [28,29] and Random Forests (RF) [30,31]. These methods improve detection accuracy and monitoring of this invasive species but struggle with the increasing complexity and volume of remote sensing data, particularly in high-resolution and multispectral imagery. The advent of deep learning, particularly with Convolutional Neural Networks (CNNs), marked a significant turning point [32]. CNNs introduced the ability to automatically extract hierarchical features from raw image data, significantly enhancing classification accuracy and efficiency [33]. However, CNNs in remote sensing image classification are limited by their inability to produce dense, pixel-level predictions [34]. This limitation is addressed by Fully Convolutional Networks (FCNs), which use fully convolutional architectures to enable precise pixel-wise segmentation [35]. Nevertheless, FCNs struggle with coastal wetlands due to their gradual transitions and unclear boundaries, leading to reduced accuracy in pixel-wise classification as spatial connections and spectral features are inadequately captured. Impressively the U-Net model, originally for biomedical image segmentation, excels in wetland remote sensing due to its symmetric encoder-decoder structure. It provides precise localization and contextual understanding by capturing high-level features and reconstructing spatial resolution [36–38]. Li, et al. [39] used U-Net with Sentinel-2A&B images for salt marsh wetlands mapping in South Carolina's estuary. Qin, et al. [40] applied U-Net to Zhuhai-1 hyperspectral images for more accurate small waterbody extraction, compared to SVM and the normalized waterbody index. Huang, et al. [41] utilized GF-2 images and U-Net model to study habitat changes and species competition in the China's Yellow and Bohai Sea Bird Nature Reserve. The U-Net model significantly enhances remote sensing classification in coastal wetlands by providing precise segmentation and detailed identification of land cover types and vegetation species, thereby further improving the accuracy of detecting invasive species.

S. alterniflora was first introduced into the YRD in late 20th century with the initial purpose of enhancing soil stabilization and increasing the ecological value of the wetlands [42]. However, due to its high growth rate and competitive nature, *S. alterniflora* rapidly colonized large areas of the delta,

outcompeting native vegetation and altering the local ecosystem. In 2020, the Department of Natural Resources of Shandong Province, along with four other departments, jointly issued the Implementation Plan for the Prevention and Control of *S. alterniflora* in Shandong Province (2020-2022), aiming to establish a replicable and promotable control model for *S. alterniflora* in China's northern intertidal zones. Building on this foundation, in 2023, Shandong Province launched the "Action Plan for the Prevention and Control of *S. alterniflora* in Shandong Province (2023-2025)", aiming to curb its growth and prevent resurgence, with the goal of eradication within three years.

Accordingly, timely and accurate monitoring of *S. alterniflora* clearance and resurgence, along with evaluating the effectiveness of control projects, is crucial for managing *S. alterniflora* and protecting coastal wetland ecological security in Shandong Province. Therefore the objectives of this study are to quantify the dynamics of *S. alterniflora* invasion during the implementation of multiple control policies in the YRD; analyze the variations in habitat patterns, interspecific competition, and the characteristics of shifts in habitat types; evaluate both the effectiveness and challenges of managing *S. alterniflora* invasion in the YRD.

2. Materials and Methods

2.1. Study Area

The YRD, situated in Eastern China, is one of the largest deltas in China, formed by the mouth of the Yellow River. The nature reserve spans approximately 1.53×10^5 hm² and is located between 37°35' and 38°12' N and 118°33' and 119°20' E (Figure 1). This region features flat terrain with fertile soil, serving as a significant agricultural zone. The sediment deposition from the Yellow River has led to the development of a unique wetland ecosystem, that supports a wide variety of flora and fauna. A typical subtropical monsoon climate prevails over the region, with the mean annual temperature and precipitation ranging from 11.7 to 12.6°C and 530 to 630 mm.

The common intertidal plants in this study area include *S. alterniflora*, *Reed*, *Suaeda*, and *Tamarisk* [43]. In 1992, the Chinese government established the Yellow River Delta National Nature Reserve (YRDNNR), the country's largest wetland nature reserve, to provide a crucial stopover and breeding habitat for globally endangered bird species. The reserve was designated as a Ramsar site on October 8, 2013, highlighting its global importance as a critical habitat. The YRD is characterized by its dynamic nature and vital ecological functions, making the preservation of its wetland resources a major focus for scientists and local authorities.

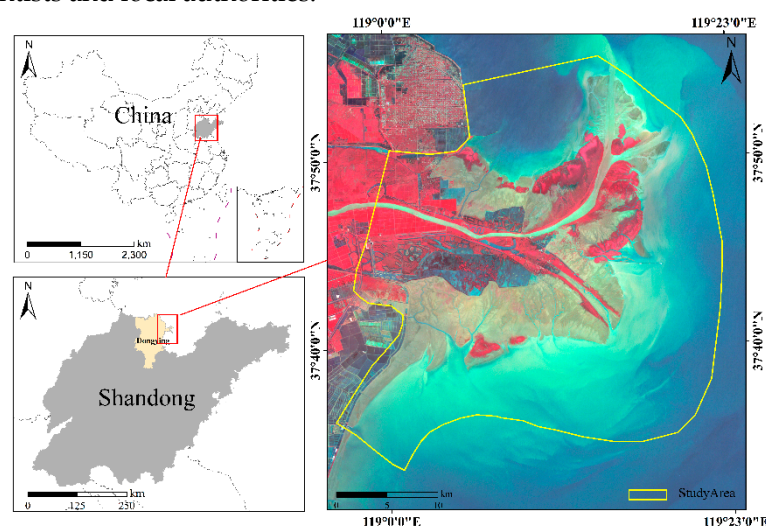


Figure 1. Locations of Study area.

2.2. Data and Processing

Hyperspectral imagery of the study area, acquired without cloud interference by Orbita Hyper Spectral (OHS) from 2019 to 2023, was downloaded from the Orbita Aerospace

(<https://www.obtdata.com/>). The Zhuhai-1 satellite constellation, operated by Zhuhai Orbit Aerospace Technology Company Ltd, is a commercial micro-nano satellite constellation with 34 satellites, with the first group launched on June 15, 2017. Currently, 12 satellites are in orbit, including four hyperspectral ones. These hyperspectral satellites—the only commercial ones in China to complete launching and networking—cover 32 bands from 400 to 1000 nm, with a spatial resolution of 10 m and a spectral resolution of 2.5 nm. The bands are uniformly distributed across the visible light and near-infrared spectrum, facilitating the extraction of diverse vegetation types by leveraging subtle spectral discrepancies between *S. alterniflora* and other vegetation species. The preprocessing of the hyperspectral images involved three steps. Initially, radiometric calibration was performed to mitigate sensor-related errors in the preprocessing of hyperspectral images. Following this, atmospheric correction was applied to the images to reduce the influence of atmospheric and radiometric factors on surface reflectance. Subsequently, orthorectification of the images was conducted to rectify geometric distortions in the original remote sensing data. Lastly, image cropping was applied to obtain the study area images. The above operations were carried out using ENVI 5.6 software.

Table 1. Parameters of Zhuhai-1 hyperspectral imagery.

Satellite Name	Imaging Sensor	Spatial Resolution	Date/Time	Cloud(%)
HCM2	CCD1	10m	20190819	3%
HDM1	COMS1	10m	20200930	1%
HEM1	CMOS2	10m	20210908	8%
HFM1	COMS2	10m	20220724	4%
HAM2	CMOS3	10m	20230930	1%

The reference data consists of a point dataset derived from ground-truth samples and visual interpretation of publicly available high-resolution historical imagery from 2019 to 2023. High-resolution images, with a spatial resolution of less than 1 m, were acquired from the Google Earth platform to support the creation of these reference datasets. During the visual interpretation of the reference points, existing literature on *S. alterniflora* mapping in the YRD [18,44] was also consulted to accurately assign land cover types to each reference point. To gather ground-truth samples, two rounds of ground surveys were conducted, one in July 2023 and another in June 2024.

2.3. Methodology

2.3.1. Feature Analysis

Spectral indices have been proved to significantly impact the accuracy of classification outcomes. To fully exploit the vegetation community characteristics embedded in hyperspectral remote sensing imagery, we extracted the spectral reflectance, the vegetation indices and texture features derived from the spectral reflectance. The first principal component of the original images contains more feature information than any single band image; therefore, the gray-level co-occurrence matrix (GLCM) texture features were extracted based on the first principal component of the original imagery. Specifically, the study utilized the GLCM method to extract eight texture features from Zhuhai-1 hyperspectral images, including mean, variance, homogeneity, dissimilarity, contrast, entropy, angular second moment, and correlation. In total, 20 spectral indices and 8 texture features were ultimately extracted.

Table 2. Formulas for vegetation and texture feature indices.

Index		Formula	Index		Formula
Spectral	NDVI	$\frac{B27 - B13}{B27 + B13}$	CCI	NDre1	$\frac{B19 - B16}{B19 + B16}$
Feature	EVI	$\frac{2.5 * (B27 - B12)}{B27 + 6 * B12 - 7.5 * B3 + 1}$	PRI	NDre2	$\frac{B22 - B16}{B22 + B16}$

NDWI	$\frac{B7 - B27}{B7 + B27}$	RVI	$\frac{B27}{B13}$	CIre	$\frac{b22}{b16} - 1$
GVI	$\frac{B27}{B7}$	DVI	$\frac{B27 - B13}{B27 + B16}$	PSRI	$\frac{b25 - B4}{B19}$
RSVI	$\frac{B27 - B13}{(B27 + B13) * B27} - \frac{B3}{B27 + B3}$	NDVIre1	$\frac{B27 - B16}{B27 + B16}$	SRredge	$\frac{B22}{B18}$
GNDVI	$\frac{B22 + B7}{B27 - B16}$	NDVIre2	$\frac{B27 + B19}{B27 - B21}$	SR1	$\frac{B27}{B13}$
MTCI	$\frac{B16 + B13}{B27 + B21}$	NDVIre3	$\frac{B27 + B21}{B27 + B21}$		
Variance	$\sum_{n=0}^{N_g-1} \sum_{j=0}^{N_g-1} (i - u)^2 p(i, j)$	Mean	$\sum_{i=0}^{N_g-1} \sum_{j=0}^{N_g-1} P(i, j) * i$		
Texture Features					
Dissimilarity	$\sum_{n=0}^{N_g-1} n \left[\sum_{i=1}^{N_g} \sum_{j=1}^{N_g} p(i, j)^2 \right]$	Contrast	$\sum_{n=0}^{N_g-1} n^2 \left[\sum_{i=1}^{N_g} cc \right]$		
Homogeneity	$\sum_{i=0}^{N_g-1} \sum_{j=0}^{N_g-1} \frac{1}{1 + (i - j)^2} p(i, j)$	Correlation	$\left[\sum_{n=0}^{N_g-1} \sum_{j=0}^{N_g-1} (ij) p(i, j) - \mu_x \mu_y \right] / \sigma_x \sigma_y$		
Angular Second Moment	$\sum_{n=0}^{N_g-1} \sum_{j=0}^{N_g-1} [p(i, j)]^2$	Entropy	$\sum_{n=0}^{N_g-1} \sum_{j=0}^{N_g-1} p(i, j) \log[p(i, j)]$		

2.3.2. Feature Selection

High-dimensional data enhance classification but increase computational costs and risk reduced accuracy due to the curse of dimensionality [45]. Thus, feature selection improves both efficiency and accuracy in multi-dimensional datasets. Relief-F is a widely used feature selection algorithm that assesses the importance of features based on their ability to differentiate between nearby instances. It operates by iteratively sampling instances from the dataset and updating the relevance scores of the features. The core idea is to find feature values that differentiate between instances of different classes especially focusing on near-hit and near-miss instances. Additionally, the algorithm is robust to interactions between features and can handle both discrete and continuous data.

Let $W[A]$ denote the weight of feature A. The update rule for the weight of feature A is given by:

$$W[A] = W[A] - \frac{1}{m} \sum_{i=1}^m \left(\frac{\text{diff}(A, R_i, \text{near}_{\text{hit}}(R_i))}{k} - \sum_{C \neq \text{class}(R_i)} \frac{P(C)}{1 - P(\text{class}(R_i))} \frac{\text{diff}(A, R_i, \text{near}_{\text{miss}}(R_i, C))}{k} \right) \quad (1)$$

Where $\text{diff}(A, R_i, N)$ measures the difference between the values of feature A for instances R_i and N , $\text{near}_{\text{hit}}(R_i)$ is the set of k nearest neighbors of R_i from the same class, $\text{near}_{\text{miss}}(R_i, C)$ is the set of k nearest neighbors of R from class C , $P(C)$ is the prior probability of class C .

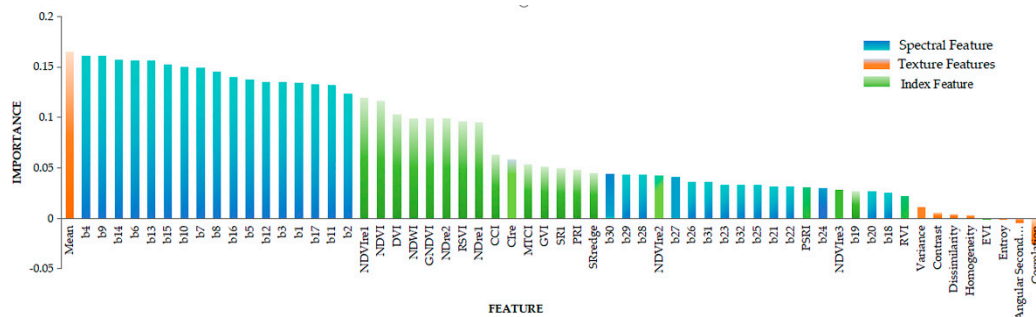


Figure 2. Relief-F feature ranking chart.





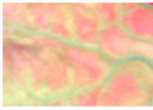

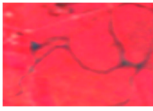



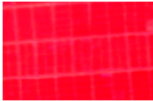


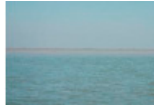
As shown in Figure 2, among the top 20 most important features, there are 17 spectral features, 2 vegetation indices and 1 texture feature. The most significant vegetation index is NDVIre1. Red-edge indices play a pivotal role in classification, consistently ranking high in importance. Meanwhile, the most important texture feature is the Mean. Conversely, among the 20 lowest-ranking features, there are 9 spectral bands, 7 texture features, and 4 vegetation indices. Overall, the importance of other texture features ranks relatively low, suggesting those features derived from 10m resolution remote sensing imagery contribute minimally to differentiating *S. alterniflora* communities from native plant communities.

To further evaluate feature significance, the ranked features were grouped into six categories. A U-Net model was then used to classify each group. By progressively adding these feature groups, the model’s classification accuracy was analyzed. This approach helped identify the optimal number of features required for accurate classification.

2.3.3. Generate the Training Data

According to field surveys and the wetland descriptions of previous literature in the YRD. The main types of wetland vegetation in the area include *S. alterniflora*, *Reed*, *Tamarix*, and *Suaeda*. In addition to these vegetation types, the region also covers with other land cover types such as water body, cropland, and tidal flat. Detailed information of the image features and classification criteria for these land cover types is provided in Table 3.

Table 3. The classification system for mapping wetlands in YRD.

Types	Image Example	Image feature	Photograph of the scene
<i>S. alterniflora</i>		These species thrive in intertidal zones, forming dense communities that appear vibrant red in images, while low coverage areas with high water content appear deep red.	
<i>Tamarix</i>		<i>Tamarix</i> shrubs, sparsely distributed and mixed with Reeds and alkali-resistant plants, thrive in high-tide areas of the intertidal zone, appearing as a dark red network in imagery.	
<i>Suaeda</i>		It exhibits a light red hue, characterized by a more uniform distribution, predominantly occupying regions with elevated salinity levels	
<i>Reed</i>		<i>Reed</i> dominate the freshwater habitat, with sparse <i>Tamarisk</i> and a decline of <i>S. alterniflora</i> , appearing as dark red shades in late autumn imagery.	
Tidal flat		Located along the high-water mark of exposed beaches, these areas appear white or light gray in imagery due to low water content, soil salinization, and strong light reflection.	
Cropland		Its form is consistent and texture fine, resulting in a bright red appearance in the imagery.	
Water body		These features include aquaculture ponds, reservoirs, rivers, and open ocean, all appearing blue in the imagery.	

Deep learning training data was generated annually using object-oriented segmentation combined with random forest classification. Following this, visual precision correction was performed on the RF classification results. First, misclassifications were identified by comparing them with high-resolution data, and manual corrections were then applied. All operations were conducted

in ArcGIS 10.9. Lastly, the corrected classified results were exported in TIFF format, which served as labels for deep learning training.

2.3.4. U-Net Training and Prediction

The U-Net model is a deep learning architecture designed for image classification, utilizing an encoder-decoder framework (Figure 3). The encoder path extracts features by reducing spatial resolution, while the decoder path restores resolution through upsampling, using skip connections to retain detailed information. This approach allows the model to effectively capture both global context and local details, making it highly suitable for pixel-level classification tasks.

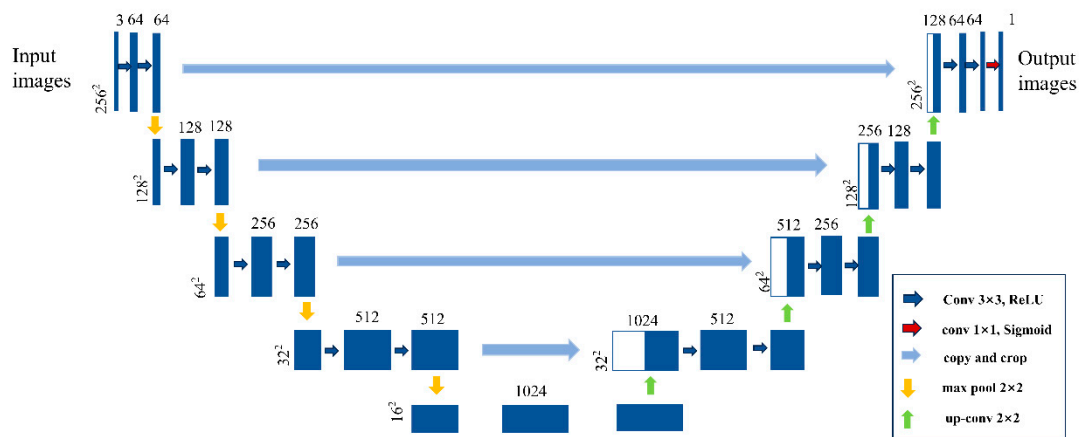


Figure 3. U-Net model structure diagram.

The composite images which covered the whole study area of the *S. alterniflora* and the training data were split into the size of 32 x 32 pixels. Three parameters should be set before training: initial learning rate, training batch size, and training epoch. Based on the previous studies and our experiments in this research, we have set the initial learning rate to 0.01, the training batch size to 8 and the training epoch to 300. Besides, two evaluation metrics, accuracy and loss, are utilized to assess the training model. The optimal model is the one with the highest accuracy value and lowest loss value.

2.3.5 Accuracy Assessment

A confusion matrix was created for annual land cover map of the YRD. We applied four evaluation metrics, i.e., producer's accuracy (PA), user's accuracy (UA), overall classification accuracy (OA), and kappa coefficient, to assess the accuracy of identified *S. alterniflora* from 2019 to 2023. The above indices were also used to evaluate the accuracy of the U-Net model in comparison with traditional machine learning models, such as SVM and RF. The specific formulas are as follows:

$$PA = \frac{X_{ij}}{X_{i*}} \quad (2)$$

$$UA = \frac{X_{ij}}{X_{*j}} \quad (3)$$

$$OA = \frac{S_d}{n} \quad (4)$$

$$Kappa = \frac{OA - \frac{\sum (X_{i*} \times X_{*j})}{n^2}}{1 - \frac{\sum (X_{i*} \times X_{*j})}{n^2}} \quad (5)$$

where X_{ij} represents the count of samples classified as land cover type i , which actually belong to land cover type j ; X_{i*} signifies the total count of samples classified as land cover type i ; X_{*j} represents the accurate count of samples correctly classified as the true land cover type j .

3. Results

3.1. Feature Selection and Accuracy Assessment

To evaluate the performance of the U-Net method, the 2020 hyperspectral image was used as an example. The original data without feature selection was classified using SVM, RF, and U-Net to compare their performance. Subsequently, the U-Net model was applied to classify multidimensional features selected through the Relief-F method to validate its effectiveness. The features ranked by importance in Section 2.3.2 were divided into six groups, and classification was conducted for each group using the U-Net model (Table 4). The results indicate that classification accuracy increases with the number of features, peaking at Group 4 with 40 features, and then gradually declining, suggesting that Group 4 is the optimal feature dataset.

Table 4. Grouping and classification accuracy.

Group	Number of Features	Classification Accuracy
1	10	0.877
2	20	0.891
3	30	0.905
4	40	0.930
5	50	0.905
6	60	0.898

Figure 4 presents the classification results of the original hyperspectral imagery using SVM, RF, SVM, and U-Net, as well as those obtained using the optimal feature dataset with the U-Net model. The land cover distribution patterns are generally consistent across the four classification schemes. However, the classification results from SVM and RF exhibit a more pronounced "salt-and-pepper" effect (Figure 4a, b). In contrast, U-Net effectively reduces this noise by capturing spatial-contextual information, thereby enhancing the quality of hyperspectral image classification. Examination of the confusion matrices for the four classification models (Table 5) reveals that U-Net achieves superior classification performance compared to SVM and RF when using the original hyperspectral imagery. Moreover, the U-Net model based on the Relief-F optimal feature dataset outperforms the U-Net method using the original hyperspectral data. This optimized U-Net model was then applied to classify imagery from 2019, 2021, 2022, and 2023, achieving an overall accuracy above 90% for each year, thus meeting the required standards.

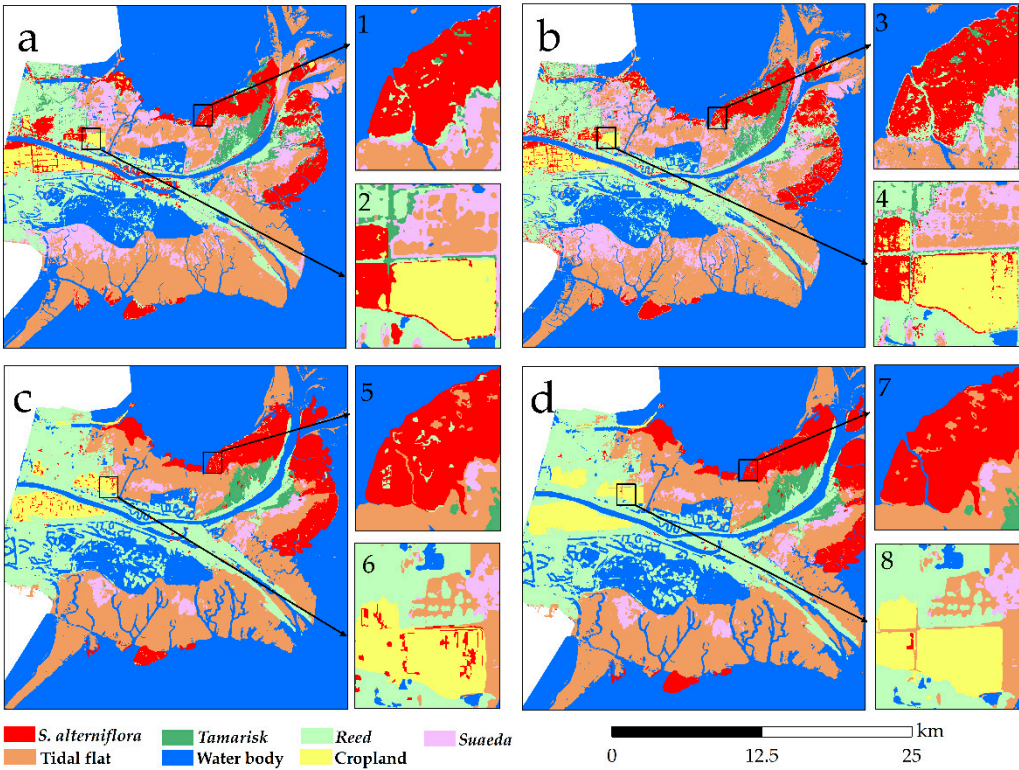


Figure 4. Comparison of image classification results from different methods in 2020. (a) SVM; (b) RF; (c) U-Net; (d) U-Net + Relief-F.

Table 5. Accuracy validation results of four different methods using confusion matrices.

	SVM		RF		U-Net		U-Net + Relief-F	
	PA	UA	PA	UA	PA	UA	PA	UA
Water body	0.860	0.895	0.870	0.936	0.903	0.880	0.931	0.984
<i>S. alterniflora</i>	0.904	0.876	0.909	0.923	0.910	0.852	0.921	0.957
Tidal flat	0.734	0.772	0.801	0.799	0.832	0.821	0.886	0.839
<i>Reed</i>	0.836	0.868	0.874	0.870	0.883	0.842	0.896	0.960
Cropland	0.946	0.835	0.946	0.815	0.940	0.930	0.934	0.919
<i>Suaeda</i>	0.959	0.859	0.961	0.874	0.930	0.879	0.935	0.891
<i>Tamarisk</i>	0.492	0.944	0.492	0.896	0.789	0.732	0.917	0.925
OA	0.859		0.878		0.913		0.930	
Kappa	0.863		0.849		0.902		0.912	

The performance of the U-Net model during training, based on the optimal feature dataset, is shown in Figure 5. As illustrated, the model demonstrated robust classification performance, with the training process converging after approximately 250 epochs and stabilizing at a loss value close to 0.01. These results indicate that the model was well-trained and achieved high classification accuracy.

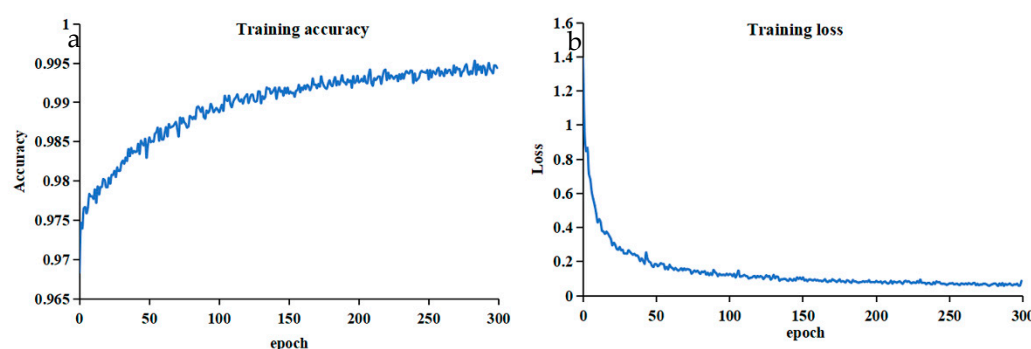


Figure 5. Curves of U-Net model accuracy and loss value. (a): Accuracy value curves; (b): Loss value curves.

3.2. Temporal and Spatial Changes of *S. alterniflora* in YRD

The maps of plant communities in the YRD provide a clear and comprehensive depiction of the distribution of main vegetation types in the study area, such as *S. alterniflora*, *Reed*, *Suaeda*, and *Tamarix* (Figure 6). In 2019, *S. alterniflora* occupied an area of 4,055.06 hm², primarily concentrated in the southeastern region of the Gudong Oilfield, extending along both banks of the Yellow River Estuary (YRE), with smaller patches located in the southern mudflat zones. *Reed* dominated the landscape in the western part of the study area, forming large, continuous patches within a 1 to 1.5 km range on both sides of the new Yellow River channel, as well as within a 500-meter range on both sides of the old river channel in the south, covering a total area of approximately 11,009.79 hm². *Suaeda* was mainly found in extensive patches throughout the intertidal zone, encompassing an area of around 2,847.96 hm². *Tamarix*, with the smallest distribution, was sparsely interspersed between the patches of *Reed* and *Suaeda*, forming narrow, belt-like strips, and covering only 617.00 hm².

Between 2019 and 2020, the area of *S. alterniflora* expansion trend was particularly noticeable in the southeastern part of the Gudong Oilfield, the southern mudflats, and along both banks of the YRE. Additionally, the connectivity between *S. alterniflora* patches strengthened, with new patches emerging in the southern mudflats, bringing the total area to 5,242.04 hm². From 2020 to 2021, the expansion of *S. alterniflora* continued, with the total area reaching 6,105.50 hm². However, from 2021 to 2022, there was a slight decline in the *S. alterniflora* area, reducing to 5,063.62 hm². This decrease was primarily concentrated in the southeastern part of the Gudong Oilfield and the southern mudflats, where the area reduced by 462.52 hm² and 147.23 hm², respectively, although inland expansion along both banks of the YRE persisted. By 2023, *S. alterniflora* had been nearly eradicated, with only small patches remaining on the eastern bank of the YRE, covering a mere 0.55 hm².

Overall, the wetlands in the YRD experienced a relatively stable period of natural succession without human interference between 2019 and 2021. In 2022, eradication experiments commenced in parts of the study area, causing a slight decrease in *S. alterniflora* area. By 2023, the species had been almost entirely eradicated.

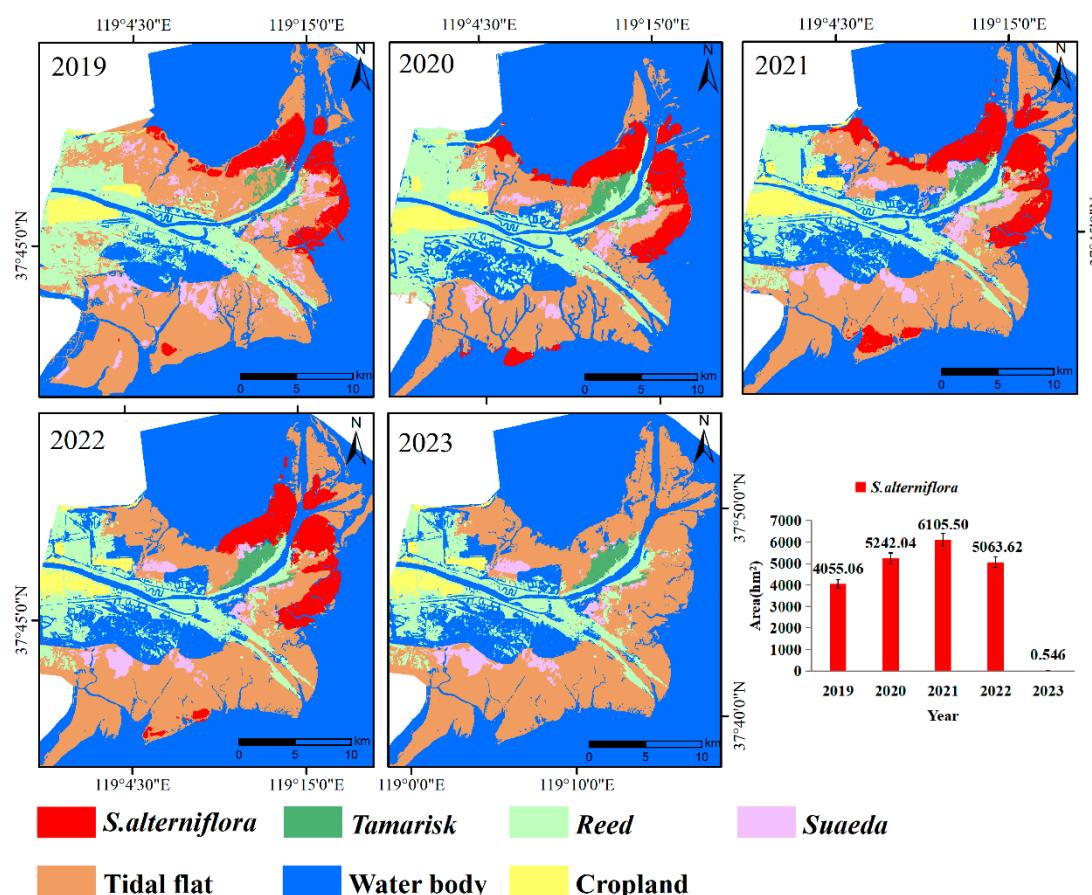


Figure 6. Spatial distribution of plant communities in the YRD and areal changes of *S. alterniflora* from 2019 to 2023.

3.3. Conversions Between *S. alterniflora* and Other Land Cover Types

To elucidate the characteristics of habitat type shifts, we analyzed the variations in habitat types across the study area and presented these findings visually. (Figure 7 and Figure 8). Between 2019 and 2020, 674.22 hm² of *S. alterniflora* were converted, mainly into water body followed by Reed areas, with transformations of 482.94 hm² and 109.88 hm², respectively. Meanwhile, the species expanded by 1862.67 hm² during this period, with the largest portion of 1144.71 hm² (61.45%) occurring on tidal flat, and 385.05 hm² and 360.42 hm² expanding into water body and *Suaeda* habitats, respectively. From 2020 to 2021, the area of *S. alterniflora* conversion experienced a slight decrease, with 637.93 hm² transformed, predominantly into water body (267.74 hm²) and tidal flat (232.56 hm²). At the same time, the species expanded by 1499.77 hm², primarily into water body (993.05 hm²) and tidal flat (335.03 hm²). In the following period, from 2021 to 2022, the species expanded by only 337.24 hm² but saw a significant reduction of 1378.99 hm², with most of the expansion occurring in water body (205.52 hm²), accounting for over 60% of the total. The reduction was concentrated on tidal flat (999.62 hm², over 70%), followed by water body (368.84 hm²). Between 2022 and 2023, *S. alterniflora* underwent a dramatic decline, with nearly all areas converted, primarily into tidal flat (4734.43 hm², 94%), and smaller portions transitioning into water body and Reed areas. Overall, from 2019 to 2023, *S. alterniflora* expanded by a total of 3699.68 hm² and contracted by 7743.05 hm². The largest expansion occurred between 2019 and 2020 (1862.67 hm²), while the most significant reduction occurred between 2022 and 2023 (5051.91 hm²).

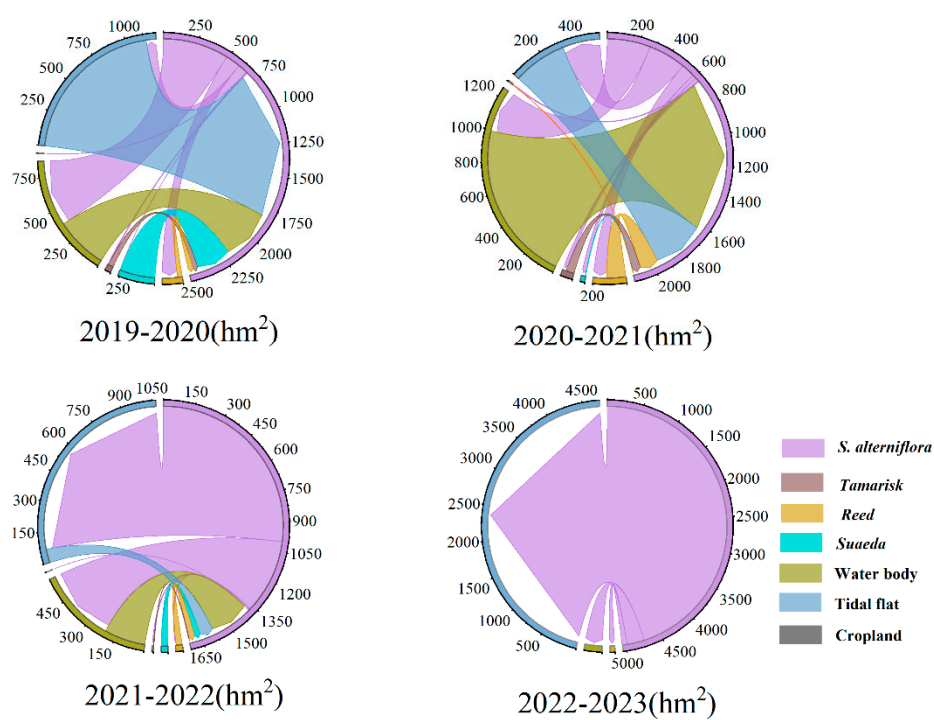


Figure 7. Transfer matrix of land use types within the study area from 2019 to 2023.

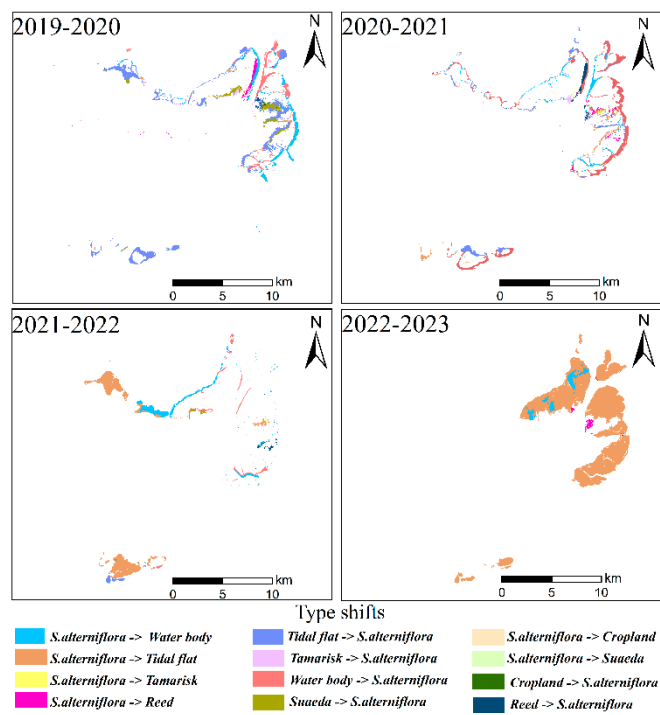


Figure 8. Spatial distribution of transitions between *S. alterniflora* and other land cover types for the four temporal intervals: 2019-2020, 2020-2021, 2021-2022 and 2022-2023.

4. Discussion

4.1. Uncertainties

When utilizing the U-Net model to extract *S. alterniflora* from Zhuhai-1 hyperspectral imagery, several uncertainties and factors can contribute to inaccuracies in the results. The first is data-related

uncertainty. *S. alterniflora* may exhibit spectral variations due to differences in plant health, growth stages, or environmental stressors [46], which can complicate consistent identification by the U-Net model. Tian et al. [14] pointed out that two stands of *S. alterniflora* in his study area were at rather different phenological stages on the same date, associated with clearly different spectral features. And the YRD exhibits diverse land cover types, there are no distinct boundaries between vegetation classes. It is impossible to label all land cover types during the sample preparation process, which may result in insufficient sample accuracy and potentially reduce classification accuracy. Misclassification may occur when other vegetation, particularly *Reed* in the YRD, display similar reflectance patterns. Although the spatial resolution of the Zhuhai-1 imagery is superior to most hyperspectral satellite data, its 10-meter resolution may still result in mixed pixels representing different plant species, especially near the edges of *S. alterniflora* patches. Additionally, variations in atmospheric conditions during image acquisition can alter the spectral data, introducing further uncertainties. For instance, the results of this study demonstrate that the classification accuracy of *S. alterniflora* in the 2020 imagery, which had better atmospheric conditions, is significantly higher than in other years.

The second type of uncertainty is model-related. A limited number of labeled examples of *S. alterniflora* can restrict the U-Net model's ability to generalize, potentially leading to overfitting or poor performance on unseen data. Inaccurate or inconsistent annotations in the training dataset can further confuse the model, resulting in incorrect extractions. While U-Net is a powerful tool for image segmentation, it may struggle with the high dimensionality of hyperspectral data if not properly adapted, potentially leading to suboptimal feature extraction [47]. In this study, we addressed this issue by using the Relief-F algorithm for feature selection and then inputting the prioritized features into the U-Net model, ultimately achieving satisfactory classification accuracy.

Moreover, environmental, temporal and external factors, such as lighting condition, phenological change and geographical variability may also increase the uncertainty of the classification. To address uncertainties and enhance accuracy in *S. alterniflora* extraction, several strategies can be applied: 1) improving data quality by using higher-resolution hyperspectral sensors and thorough preprocessing to minimize noise and atmospheric distortions; 2) expanding and diversifying the training dataset with more labeled samples and data augmentation techniques; 3) adapting the U-Net model to handle high-dimensional data through dimensionality reduction or attention mechanisms; 4) employing robust validation methods such as cross-validation and using diverse datasets to ensure generalization; and 5) incorporating multi-temporal images to account for phenological variations and strengthen the model's robustness.

4.2. Policies and Measures to Control *S. alterniflora* Invasion in YRD

Studies on the control of *S. alterniflora* have been reported across Asia [48], North America [49], Europe [50], and Africa [51], with a primary focus on China [52,53] and the United States [39]. In China, most research is concentrated in Shanghai [54] and Fujian provinces [55], where at least seven control methods have been tested. As one of the earliest introduced invasive alien species, *S. alterniflora* poses a serious threat to China's ecosystems. In response, the Chinese government has formulated policies and implemented various measures aimed at controlling its spread and restoring damaged ecosystems. Shandong Province, one of the regions most severely affected by the invasion, has responded actively by formulating and implementing targeted control measures (Figure 9). These efforts, under national policy guidance, combine physical, chemical, and biological methods to effectively curb the spread of *S. alterniflora* and restore the local wetland ecosystem.

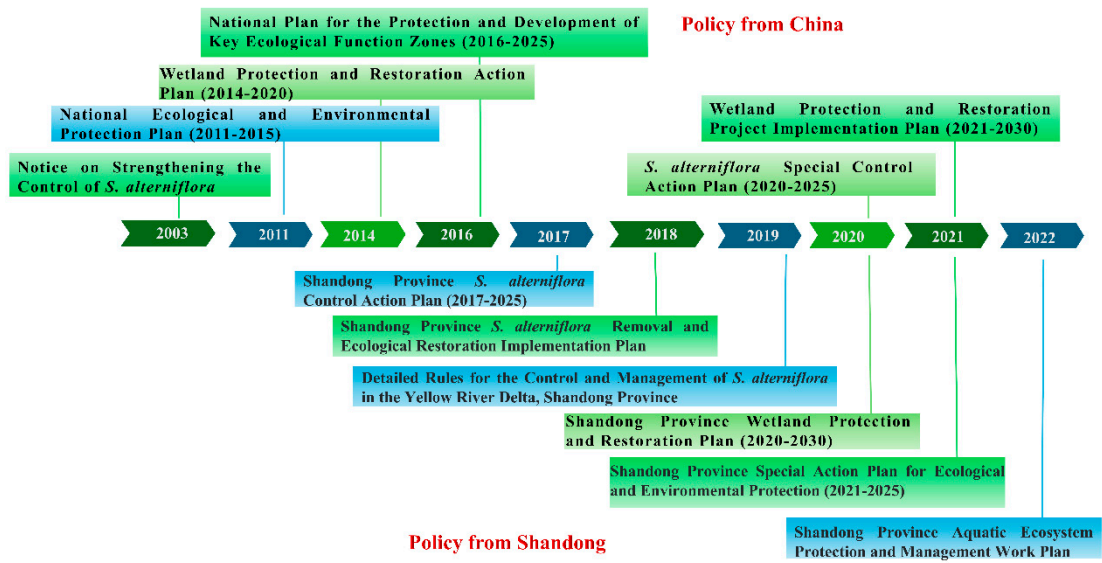


Figure 9. Overview of *S. alterniflora* management policies issued by China and Shandong province.

First, physical methods such as mowing and flooding are the primary techniques used. In the mowing method, Qiao [56] conducted two rounds of close-to-ground mowing on July 12 and July 27 at the YRD, leaving stubble heights of 2-3 cm. By October of the same year, *S. alterniflora* density had decreased by 99.8%. In the flooding method [57], seedlings (5-7 cm tall) that had germinated in May were subjected to continuous flooding at depths of 10-20 cm. After 43 days, both flooding depths achieved 100% control of the seedlings. These physical techniques are highly effective in eliminating seedlings, but less effective against mature *S. alterniflora*. Repeated manual removal or mowing can yield better results. Second, chemical control, guided by the "Implementation Plan for *S. alterniflora* Removal and Ecological Restoration in Shandong Province," involves the use of eco-friendly herbicides such as glyphosate. In trials conducted at the YRD in June and July 2019, Xie et al. [57] tested three chemical application rates: 4, 8, and 12 kg/hm². Observations in May of the following year showed eradication rates of 16.1%, 23.4%, and 22.4%, respectively. While chemical methods are simple and effective, they may pose environmental risks. Some studies [58,59] have found no detectable herbicide residues in seawater, sediments, or organisms like clams, but these were conducted in small areas where tidal movements may have washed residues away shortly after application. In biological control, pilot projects have tested the introduction of natural enemies or pathogens to control *S. alterniflora*. However, research in this area is limited. For example, researchers [60–62] attempted to use the *Littoraria irrorata* to control *S. alterniflora*, but the results were not promising. Finally, Shandong Province has also adopted integrated control measures [57,63]. One example is the "mowing-flooding" method, where *S. alterniflora* is mowed to a height of less than 2 cm in early June or August, followed by continuous flooding at depths of 20, 30, or 40 cm. Surveys conducted from November of the same year to the following year showed control efficiencies of 99%-100%. Another method, "mowing-plowing," involves plowing the area to a depth of 20 cm in October. A survey conducted in June of the following year showed a control efficiency of 99%. Integrated techniques, which generally outperform single methods, can be applied in both salt marsh and mangrove wetland ecosystems.

Since 2020, the YRD has invested approximately 500 million yuan in controlling *S. alterniflora*. By 2023, the area of *S. alterniflora* in the study region had been reduced to just 0.50 hm², demonstrating the effectiveness of these measures in curbing its spread. Following the implementation of these policies, *S. alterniflora* in the YRD was largely eradicated, with a removal rate of 99.99% by 2023. However, during a field survey in the study area (37.796634°N, 119.154673°E), our team still detected signs of regrowth. This finding indicates that although previous control measures successfully inhibited the spread and growth of *S. alterniflora*, its robust root system and strong survival capabilities pose a risk of regrowth. Therefore, long-term monitoring and maintenance are crucial to ensure that regrowth is promptly identified and managed, preventing further large-scale spread and

ensuring the complete restoration and stability of wetland ecosystems. The results of this study demonstrate that the management of *S. alterniflora* in the YRD has led to notable success, with significant reductions in the invasive species' spread.

4.3. Future Managements of *S. alterniflora*

The future management of *S. alterniflora* in the YRD will focus on sustaining the successes achieved thus far through continuous monitoring, early detection, and prevention of re-invasion. Our research indicates that as of 2023, approximately 0.5hm² of *S. alterniflora* remain in the YRD. Given the species' high adaptability to climatic and environmental conditions, strong reproductive capacity, salt tolerance, and flood resilience, it poses a significant challenge to complete eradication. The species propagates rapidly through seeds, rhizomes, and asexual fragments, making any residual seeds or rhizomes potential sources for re-establishment [52].

To address these challenges, post-eradication efforts must prioritize the restoration of native vegetation and the rehabilitation of wetland ecosystems. Replanting indigenous species that can outcompete *S. alterniflora* is crucial for restoring ecological balance and enhancing the resilience of the wetland environment [53]. Implementing continuous monitoring and early detection systems is essential to prevent re-invasion. Advanced remote sensing technologies, including unmanned aerial vehicles (UAVs) and high-resolution satellite imagery, will play a critical role in tracking the species' spread and assessing the effectiveness of control measures [41]. Incorporating multi-temporal imagery can also account for phenological variations, strengthening the robustness of monitoring efforts.

Engaging local communities and raising public awareness about the impact of *S. alterniflora* are vital components of sustainable management. Public participation in removal efforts and ecosystem restoration projects can significantly enhance the effectiveness of management strategies [20]. Educational programs and community outreach can foster a sense of stewardship and encourage proactive involvement in conservation initiatives. Ongoing research should focus on developing innovative and more effective control techniques, such as utilizing biological control agents or novel chemical formulations with minimal environmental impact [48]. Collaboration with scientific institutions and environmental organizations will drive innovation in managing this invasive species. Additionally, integrating machine learning algorithms and artificial intelligence into monitoring programs can improve the accuracy of species identification and prediction of invasion patterns [33].

Strengthening policies and regulations related to invasive species management is crucial to ensure that control measures are consistently applied. This includes enforcing restrictions on activities that might facilitate the spread of *S. alterniflora*, such as unregulated coastal development or aquaculture practices, and providing clear guidelines for land use in affected areas [55]. International cooperation may also be beneficial, given the global nature of invasive species spread, to share best practices and coordinate efforts across regions. Moreover, after the completion of control projects, regular monitoring should be conducted to promptly detect and eradicate any residual or secondary invasions of *S. alterniflora*. Adaptive management strategies should be employed, allowing for adjustments based on monitoring results and changing environmental conditions. Measures such as local vegetation restoration and tidal flat utilization should be implemented to consolidate the results of control efforts. In suitable areas, planting fast-growing mangroves or engaging in tidal flat aquaculture can enhance ecosystem resilience and provide additional economic benefits to local communities [63]. Evaluating the effectiveness of *S. alterniflora* control measures and assessing environmental impacts are necessary for informing future management strategies. This includes establishing metrics for success, such as reductions in *S. alterniflora* coverage, improvements in biodiversity, and restoration of ecosystem services. Environmental impact assessments can ensure that control methods do not adversely affect non-target species or habitat quality.

In summary, the future management of *S. alterniflora* in the YRD will be characterized by a comprehensive, science-based approach that integrates various control methods, restores native ecosystems, and involves local communities in the long-term sustainability of the region. Continuous monitoring, adaptive management, and collaborative efforts among stakeholders will be essential to prevent re-invasion and ensure the complete restoration and stability of wetland ecosystems.

5. Conclusions

In response to the escalating invasion of *S. alterniflora* in the coastal salt marshes of the YRD, acquiring accurate and timely data on its spatial and temporal dynamics is imperative for effective ecosystem management and ecological conservation. This study employed multiple classification methods—including RF, SVM, U-Net, and U-Net enhanced with the Relief-F algorithm to classify the invasive *S. alterniflora* within the coastal wetlands of the YRD. Comparative analysis revealed that the U-Net model augmented with the Relief-F feature selection algorithm achieved the highest accuracy and precision in mapping *S. alterniflora*. Utilizing this optimized method, we obtained geospatial data reflecting its annual distribution from 2019 to 2023 at a spatial resolution of 10 meters.

The results indicated a consistent expansion of *S. alterniflora* from 2019 to 2021, particularly in coastal areas, primarily encroaching upon tidal flats and water bodies, which accounted for over 80% of the expansion area. However, due to intensive removal efforts initiated in 2022, a significant decline in its coverage was observed, with the area further reduced by 2023 to approximately 0.55 hectares, achieving a 99.9% removal rate. This reduction predominantly converted back to tidal flats and water bodies, demonstrating the effectiveness of these management measures. These findings enhance our understanding of *S. alterniflora*'s growth patterns and its impact on the coastal wetland ecosystem of the YRD. The successful application of advanced remote sensing techniques and machine learning models underscores the potential for technology-driven approaches in ecological monitoring and invasive species management.

Looking forward, future research should focus on developing more sophisticated monitoring systems that integrate multi-source data, including higher-resolution imagery and in-situ observations, to detect early signs of *S. alterniflora* resurgence. Additionally, exploring the ecological implications of its removal on native species and ecosystem functions will be crucial for restoring and maintaining the health and resilience of this critical ecosystem. Collaboration among policymakers, scientists, and local communities will be essential to implement adaptive management strategies that not only control *S. alterniflora* but also enhance biodiversity and ecosystem services in the YRD. The methodologies and insights gained from this study can serve as a model for managing invasive species in other coastal wetlands globally, contributing to broader efforts in environmental conservation and sustainable development.

Author Contributions: Conceptualization, H.L. (Huiying Li) and G.C.; methodology, H.L. (Huiying Li) and G.C.; software, H.L. (Huiying Li), G.C., Q.W. and H.L. (Haojie Liu); validation, H.L. (Haojie Liu) and S.Z.; formal analysis, G.C.; investigation, H.L. (Huiying Li), G.C., Q.W. and H.L. (Haojie Liu); resources, H.L. (Huiying Li) and M.J.; data curation, H.L. (Huiying Li) and G.C.; writing—original draft preparation, H.L. (Huiying Li) and G.C.; writing—review and editing, G.C., H.L. (Huiying Li), X.H. and R.Z.; visualization, H.L. (Huiying Li) and G.C.; supervision, H.L. (Huiying Li), X.H. and R.Z.; project administration, H.L. (Huiying Li), M.J., D.M., H.Y. and Z.W.; funding acquisition, H.L. (Huiying Li), M.J., D.M., H.Y. and Z.W. All authors have read and agreed to the published version of the manuscript.

Funding: This study was funded by The National Natural Science Foundation of China (42330109, 42101399, 42001383), the Natural Science Foundation of Shandong province (No. ZR2020QD020), the Open Project Program of Fujian Key Laboratory of Big Data Application and Intellectualization for Tea Industry, Wuyi University (FKLBDAIT202303).

Data Availability Statement: The data presented in this study are available upon request from the first author.

Conflicts of Interest: The authors declare no competing interests.

References

1. MEa, M.E.A. Ecosystems and Human Well-Being: wetlands and water synthesis. 2005.
2. Wang, Z.; Wu, J.; Madden, M.; Mao, D. China's wetlands: conservation plans and policy impacts. *Ambio* 2012, 41, 782-786.
3. Yan, D.; Li, J.; Yao, X.; Luan, Z. Quantifying the long-term expansion and dieback of *Spartina alterniflora* using google earth engine and object-based hierarchical random forest classification. *IEEE J. Sel. Top. Appl. Earth Obs. Remote Sens.* 2021, 14, 9781-9793.
4. Hou, X.; Wu, T.; Hou, W.; Chen, Q.; Wang, Y.; Yu, L. Characteristics of coastline changes in mainland China since the early 1940s. *Science China Earth Sciences* 2016, 59, 1791-1802.
5. Civile, J.C.; Sayce, K.; Smith, S.D.; Strong, D.R. Reconstructing a century of *Spartina alterniflora* invasion with historical records and contemporary remote sensing. *Ecoscience* 2005, 12, 330-338.

6. Zhu, W.; Ren, G.; Wang, J.; Wang, J.; Hu, Y.; Lin, Z.; Li, W.; Zhao, Y.; Li, S.; Wang, N. Monitoring the Invasive Plant *Spartina alterniflora* in Jiangsu Coastal Wetland Using MRCNN and Long-Time Series Landsat Data. *Remote Sens.* 2022, 14, doi:10.3390/rs14112630.
7. Yan, D.; Li, J.; Xie, S.; Liu, Y.; Sheng, Y.; Luan, Z. Examining the expansion of *Spartina alterniflora* in coastal wetlands using an MCE-CA-Markov model. *Frontiers in Marine Science* 2022, 9, doi:10.3389/fmars.2022.964172.
8. Ren, G.-B.; Wang, J.-J.; Wang, A.-D.; Wang, J.-B.; Zhu, Y.-L.; Wu, P.-Q.; Ma, Y.; Zhang, J. Monitoring the invasion of smooth cordgrass *Spartina alterniflora* within the modern Yellow River Delta using remote sensing. *J. Coast. Res.* 2019, 90, 135-145.
9. Zhou, H.-X.; Liu, J.-e.; Qin, P. Impacts of an alien species (*Spartina alterniflora*) on the macrobenthos community of Jiangsu coastal inter-tidal ecosystem. *Ecol. Eng.* 2009, 35, 521-528.
10. Müllerová, J.; Pergl, J.; Pyšek, P. Remote sensing as a tool for monitoring plant invasions: Testing the effects of data resolution and image classification approach on the detection of a model plant species *Heracleum mantegazzianum* (giant hogweed). *Int. J. Appl. Earth Obs. Geoinf.* 2013, 25, 55-65.
11. Lü, J.; Jiang, W.; Wang, W.; Chen, K.; Deng, Y.; Chen, Z.; Li, Z. Wetland landscape pattern change and its driving forces in Beijing-Tianjin-Hebei region in recent 30 years. *Acta Ecologica Sinica* 2018, 38, 4492-4503.
12. Liu, X.; Liu, H.; Gong, H.; Lin, Z.; Lv, S. Applying the one-class classification method of maxent to detect an invasive plant *Spartina alterniflora* with time-series analysis. *Remote Sens.* 2017, 9, 1120.
13. Gong, Z.; Zhang, C.; Zhang, L.; Bai, J.; Zhou, D. Assessing spatiotemporal characteristics of native and invasive species with multi-temporal remote sensing images in the Yellow River Delta, China. *Land Degrad. Dev.* 2021, 32, 1338-1352.
14. Tian, J.; Wang, L.; Yin, D.; Li, X.; Diao, C.; Gong, H.; Shi, C.; Menenti, M.; Ge, Y.; Nie, S. Development of spectral-phenological features for deep learning to understand *Spartina alterniflora* invasion. *Remote Sens. Environ.* 2020, 242, 111745.
15. Xie, T.; Li, S.; Cui, B.; Bai, J.; Wang, Q.; Shi, W. Rainfall variation shifts habitat suitability for seedling establishment associated with tidal inundation in salt marshes. *Ecol. Indic.* 2019, 98, 694-703.
16. Xie, T.; Cui, B.; Li, S.; Zhang, S. Management of soil thresholds for seedling emergence to re-establish plant species on bare flats in coastal salt marshes. *Hydrobiologia* 2019, 827, 51-63.
17. Ozesmi, S.L.; Bauer, M.E. Satellite remote sensing of wetlands. *Wetl. Ecol. Manag.* 2002, 10, 381-402.
18. Qiu, Z.; Mao, D.; Feng, K.; Wang, M.; Xiang, H.; Wang, Z. High-resolution mapping changes in the invasion of *Spartina Alterniflora* in the Yellow River Delta. *IEEE J. Sel. Top. Appl. Earth Obs. Remote Sens.* 2022, 15, 6445-6455.
19. Chen, M.; Ke, Y.; Bai, J.; Li, P.; Lyu, M.; Gong, Z.; Zhou, D. Monitoring early stage invasion of exotic *Spartina alterniflora* using deep-learning super-resolution techniques based on multisource high-resolution satellite imagery: A case study in the Yellow River Delta, China. *Int. J. Appl. Earth Obs. Geoinf.* 2020, 92, 102180, doi:https://doi.org/10.1016/j.jag.2020.102180.
20. Zuo, P.; Zhao, S.; Liu, C.a.; Wang, C.; Liang, Y. Distribution of *Spartina* spp. along China's coast. *Ecol. Eng.* 2012, 40, 160-166.
21. Wang, X.; Xiao, X.; Zhang, X.; Wu, J.; Li, B. Rapid and large changes in coastal wetland structure in China's four major river deltas. *Global Change Biology* 2023, 29, 2286-2300.
22. Liu, M.; Li, H.; Li, L.; Man, W.; Jia, M.; Wang, Z.; Lu, C. Monitoring the invasion of *Spartina alterniflora* using multi-source high-resolution imagery in the Zhangjiang Estuary, China. *Remote Sens.* 2017, 9, 539.
23. Kuenzer, C.; Bluemel, A.; Gebhardt, S.; Quoc, T.V.; Dech, S. Remote Sensing of Mangrove Ecosystems: A Review. *Remote Sens.* 2011, 3, 878-928, doi:10.3390/rs3050878.
24. Hirano, A.; Madden, M.; Welch, R.J.W. Hyperspectral image data for mapping wetland vegetation. 2003, 23, 436-448.
25. Yan, D.; Li, J.; Yao, X.; Luan, Z.J.S.o.T.T.E. Integrating UAV data for assessing the ecological response of *Spartina alterniflora* towards inundation and salinity gradients in coastal wetland. 2022, 814, 152631.
26. Stuart, M.B.; McGonigle, A.J.; Willmott, J.R. Hyperspectral imaging in environmental monitoring: A review of recent developments and technological advances in compact field deployable systems. *Sensors* 2019, 19, 3071.
27. Wang, X.; Wang, L.; Tian, J.; Shi, C. Object-based spectral-phenological features for mapping invasive *Spartina alterniflora*. *Int. J. Appl. Earth Obs. Geoinf.* 2021, 101, 102349.
28. Liu, X.; Liu, H.; Datta, P.; Frey, J.; Koch, B. Mapping an invasive plant *Spartina alterniflora* by combining an ensemble one-class classification algorithm with a phenological NDVI time-series analysis approach in middle coast of Jiangsu, China. *Remote Sens.* 2020, 12, 4010.
29. Li, H.; Mao, D.; Wang, Z.; Huang, X.; Li, L.; Jia, M. Invasion of *Spartina alterniflora* in the coastal zone of mainland China: Control achievements from 2015 to 2020 towards the Sustainable Development Goals. *J. Environ. Manag.* 2022, 323, 116242, doi:https://doi.org/10.1016/j.jenvman.2022.116242.

30. Tian, Y.; Jia, M.; Wang, Z.; Mao, D.; Du, B.; Wang, C. Monitoring invasion process of *Spartina alterniflora* by seasonal Sentinel-2 imagery and an object-based random forest classification. *Remote Sens.* 2020, 12, 1383.
31. Van Beijma, S.; Comber, A.; Lamb, A. Random forest classification of salt marsh vegetation habitats using quad-polarimetric airborne SAR, elevation and optical RS data. *Remote Sens. Environ.* 2014, 149, 118-129.
32. Hinton, G.E.; Osindero, S.; Teh, Y.-W. A fast learning algorithm for deep belief nets. *Neural Comput.* 2006, 18, 1527-1554.
33. Li, Y.; Zhang, H.; Xue, X.; Jiang, Y.; Shen, Q. Deep learning for remote sensing image classification: A survey. *Wiley Interdisciplinary Reviews: Data Mining and Knowledge Discovery* 2018, 8, e1264.
34. Kaili, C.; Xiaoli, Z. An improved res-unet model for tree species classification using airborne high-resolution images. *Remote Sens.* 2020, 12, 1128.
35. Long, J.; Shelhamer, E.; Darrell, T. Fully convolutional networks for semantic segmentation. In *Proceedings of the Proceedings of the IEEE conference on computer vision and pattern recognition*, 2015; pp. 3431-3440.
36. Maggiori, E.; Tarabalka, Y.; Charpiat, G.; Alliez, P. Convolutional neural networks for large-scale remote-sensing image classification. *IEEE Transactions on geoscience and remote sensing* 2016, 55, 645-657.
37. Sharma, A.; Liu, X.; Yang, X.; Shi, D. A patch-based convolutional neural network for remote sensing image classification. *Neural Netw.* 2017, 95, 19-28.
38. Stoian, A.; Poulain, V.; Inglada, J.; Poughon, V.; Derksen, D. Land cover maps production with high resolution satellite image time series and convolutional neural networks: Adaptations and limits for operational systems. *Remote Sens.* 2019, 11, 1986.
39. Li, H.; Wang, C.; Cui, Y.; Hodgson, M. Mapping salt marsh along coastal South Carolina using U-Net. *ISPRS J. Photogramm. Remote Sens.* 2021, 179, 121-132, doi:10.1016/j.isprsjprs.2021.07.011.
40. Qin, P.; Cai, Y.; Wang, X. Small Waterbody Extraction With Improved U-Net Using Zhuhai-1 Hyperspectral Remote Sensing Images. *IEEE Geoscience and Remote Sensing Letters* 2022, 19, 1-5, doi:10.1109/lgrs.2020.3047918.
41. Huang, Y.; Liu, Z.; Zheng, G.; Zhao, C. Identification of *Spartina alterniflora* habitat expansion in a *Suaeda salsa* dominated coastal wetlands. *Ecol. Indic.* 2022, 145, doi:10.1016/j.ecolind.2022.109704.
42. Shi, D.; Tian, J.; Chen, Y.J.J.o.B.U. Biological and ecological characteristics of an invasive alien species *Spartina* in Yellow River Delta. 2009, 25, 27-32.
43. Zhang, C.; Gong, Z.; Qiu, H.; Zhang, Y.; Zhou, D. Mapping typical salt-marsh species in the Yellow River Delta wetland supported by temporal-spatial-spectral multidimensional features. *Sci. Total Environ.* 2021, 783, 147061, doi:10.1016/j.scitotenv.2021.147061.
44. Pang, B.; Xie, T.; Ning, Z.; Cui, B.; Zhang, H.; Wang, X.; Gao, F.; Zhang, S.; Lu, Y. Invasion patterns of *Spartina alterniflora*: Response of clones and seedlings to flooding and salinity—A case study in the Yellow River Delta, China. *Sci. Total Environ.* 2023, 877, 162803.
45. Ren, J.S.; Wang, R.X.; Liu, G.; Feng, R.Y.; Wang, Y.N.; Wu, W. Partitioned Relief-F Method for Dimensionality Reduction of Hyperspectral Images. *Remote Sens.* 2020, 12, doi:10.3390/rs12071104.
46. Ouyang, Z.-T.; Gao, Y.; Xie, X.; Guo, H.-Q.; Zhang, T.-T.; Zhao, B. Spectral discrimination of the invasive plant *Spartina alterniflora* at multiple phenological stages in a saltmarsh wetland. *PLoS ONE* 2013, 8, e67315.
47. Su, Z.; Li, W.; Ma, Z.; Gao, R. An improved U-Net method for the semantic segmentation of remote sensing images. *Applied Intelligence* 2022, 52, 3276-3288.
48. Maebara, Y.; Tamaoki, M.; Iguchi, Y.; Nakahama, N.; Hanai, T.; Nishino, A.; Hayasaka, D. Genetic diversity of invasive *Spartina alterniflora* Loisel.(Poaceae) introduced unintentionally into Japan and its invasion pathway. *Frontiers in Plant Science* 2020, 11, 556039, doi:556039.
49. Roberts, A.; Pullin, A.S. The effectiveness of management interventions for the control of *Spartina* species: a systematic review and meta-analysis. *Aquatic Conservation: Marine and Freshwater Ecosystems* 2008, 18, 592-618.
50. Nehring, S.; Hesse, K.-J. Invasive alien plants in marine protected areas: the *Spartina anglica* affair in the European Wadden Sea. *Biol. Invasions* 2008, 10, 937-950, doi:10.1007/s10530-008-9244-z.
51. Adams, J.; van Wyk, E.; Riddin, T. First record of *Spartina alterniflora* in southern Africa indicates adaptive potential of this saline grass. *Biol. Invasions* 2016, 18, 2153-2158, doi:10.1007/s10530-015-0957-5.
52. An, S.Q.; Gu, B.H.; Zhou, C.F.; Wang, Z.S.; Deng, Z.F.; Zhi, Y.B.; Li, H.L.; Chen, L.; Yu, D.H.; Liu, Y.H. *Spartina* invasion in China: implications for invasive species management and future research. *Weed Research* 2007, 47, 183-191, doi:10.1111/j.1365-3180.2007.00559.x.
53. Liu, W.; Maung-Douglass, K.; Strong, D.R.; Pennings, S.C.; Zhang, Y. Geographical variation in vegetative growth and sexual reproduction of the invasive *Spartina alterniflora* in China. *J. Ecol.* 2016, 104, 173-181, doi:https://doi.org/10.1111/1365-2745.12487.
54. Li, H.; Zhang, L. An experimental study on physical controls of an exotic plant *Spartina alterniflora* in Shanghai, China. *Ecol. Eng.* 2008, 32, 11-21, doi:https://doi.org/10.1016/j.ecoleng.2007.08.005.

55. Li, N.; Li, L.; Zhang, Y.; Wu, M. Monitoring of the invasion of *Spartina alterniflora* from 1985 to 2015 in Zhejiang Province, China. *BMC Ecol.* 2020, 20, 7, doi:10.1186/s12898-020-00277-8.
56. Qiao, P. Study on Mechanical and Chemical Control of Invasive Plant *Spartina alterniflora* in Yellow River Delta. Hohhot: Inner Mongolia University, 2019 2019.
57. Xie, B.; Han, G.; Qiao, P.; Mei, B.; Wang, Q.; Zhou, Y.; Zhang, A.; Song, W.; Guan, B. Effects of mechanical and chemical control on invasive *Spartina alterniflora* in the Yellow River Delta, China. *PeerJ* 2019, 7, e7655, doi:10.7717/peerj.7655.
58. Zhao, Z.-y.; Xu, Y.; Yuan, L.; Li, W.; Zhu, X.-j.; Zhang, L.-q. Emergency control of *Spartina alterniflora* re-invasion with a chemical method in Chongming Dongtan, China. *Water Science and Engineering* 2020, 13, 24-33, doi:https://doi.org/10.1016/j.wse.2020.03.001.
59. Liang, Q.; Yan, Z.; Li, X. Influence of the herbicide haloxyfop-R-methyl on bacterial diversity in rhizosphere soil of *Spartina alterniflora*. *Ecotoxicol. Environ. Saf.* 2020, 194, 110366, doi:https://doi.org/10.1016/j.ecoenv.2020.110366.
60. Wu, M.-Y.; Hacker, S.; Ayres, D.; Strong, D.R. Potential of *Prokelisia* spp. as Biological Control Agents of English Cordgrass, *Spartina anglica*. *Biol. Control* 1999, 16, 267-273, doi:10.1006/bcon.1999.0752.
61. Fisher, A.J.; DiTomaso, J.M.; Gordon, T.R. Intraspecific groups of *Claviceps purpurea* associated with grass species in Willapa Bay, Washington, and the prospects for biological control of invasive *Spartina alterniflora*. *Biol. Control* 2005, 34, 170-179, doi:https://doi.org/10.1016/j.biocontrol.2005.04.014.
62. Silliman, B.R.; Zieman, J.C. Top-down control of *Spartina alterniflora* production by periwinkle grazing in a Virginia salt marsh. *ECOLOGY* 2001, 82, 2830-2845, doi:10.2307/2679964.
63. Wang, S.Y.; Martin, P.A.; Hao, Y.; Sutherland, W.J.; Shackelford, G.E.; Wu, J.H.; Ju, R.T.; Zhou, W.N.; Li, B. A global synthesis of the effectiveness and ecological impacts of management interventions for *Spartina* species. *Frontiers of Environmental Science & Engineering* 2023, 17, doi:10.1007/s11783-023-1741-x.

Disclaimer/Publisher's Note: The statements, opinions and data contained in all publications are solely those of the individual author(s) and contributor(s) and not of MDPI and/or the editor(s). MDPI and/or the editor(s) disclaim responsibility for any injury to people or property resulting from any ideas, methods, instructions or products referred to in the content.